

A system analysis of a compliant UWB IEEE 802.15.4z transmitter and receiver

Luis O. Díaz Cueva
Institute for Applied Microelectronics
(IUMA)
University of Las Palmas de Gran
Canaria
Las Palmas de Gran Canaria, Spain
luis.diaz115@alu.ulpgc.es

Dr. Javier del Pino Suárez
Institute for Applied Microelectronics
(IUMA)
University of Las Palmas de Gran
Canaria
Las Palmas de Gran Canaria, Spain
jpino@iuma.ulpgc.es

Dr. Sunil Khemchandani Lalchand
Institute for Applied Microelectronics
(IUMA)
University of Las Palmas de Gran
Canaria
Las Palmas de Gran Canaria, Spain
sunil@iuma.ulpgc.es

Abstract - This paper presents an analysis of a transmission and reception system to functionally implement an impulse radio ultra-wideband (IR-UWB) transceiver compliant with IEEE 802.15.4z standard. Main specifications related to UWB transceivers, including power density masks, frequency bands, modulation types, transmission modes, and sensitivity levels are presented. Different types of UWB pulses are defined and compared. A detailed study of different IR-UWB transmitter and receiver architectures is conducted, making emphasis on those compliant with the IEEE 802.15.4z standard for indoor positioning and precise ranging. From these architectures a functional design of transmitter and receiver is carried out in ADS Keysight, discussing further the simulation results. The transmitter allows reconfigurability of pulses shape, by means of which several pulse shapes are generated, obtaining the best sidelobe suppression 41.09 dB through a Gaussian pulse for a theoretical spectral efficiency of 94.57% with 637 MHz UWB bandwidth. For the designed receiver architecture, a flat frequency response is obtained in the interest baseband, like that of a fifth-order Gaussian filter to 6 dB. Also, a nearly constant group delay across the entire baseband is achieved, which theoretically allows receive IR-UWB pulse without distortion it.

Keywords - Impulse Radio Ultra-Wideband (IR-UWB) transceiver, IEEE 802.15.4z standard, precise ranging, UWB pulses, pulse reconfigurability, Gaussian pulse, sidelobe suppression, group delay.

I. INTRODUCTION

UWB is a short-range communication technology used for data transfer with various purposes, including indoor positioning of persons and objects, wireless sensor communication and access control. UWB is mainly characterized by its wide bandwidth, low power consumption, and precision ranging.

The IEEE 802.15.4z standard enables the implementation of indoor positioning for objects or people through precise ranging.

In 2002, the Federal Communications Commission (FCC) of the United States released frequency bands from 3.1 to 10.6 GHz, allowing their commercial and unlicensed use under certain conditions. In 2007, the UWB mask was established at the European level, establishing a maximum effective isotropic radiated power (EIRP) density of -41.3 dBm/MHz for the frequency range 6 to 8.5 GHz [1].

Fig. 1 shows the European Communications Committee (ECC) mask, and the mask released by the FCC of the United States for indoor use, displaying the frequency ranges of

UWB along with their respective permitted low power densities (dBm/MHz).

Fig. 2 illustrates the power spectral density of UWB compared to existing current technologies (Wi-Fi, Bluetooth, GPS), where it shows that the UWB maximum allowed power level is close to the noise floor for wireless communications. This implies that UWB can coexist in these bands with these technologies that are already commercially exploited without interfering with them [2].

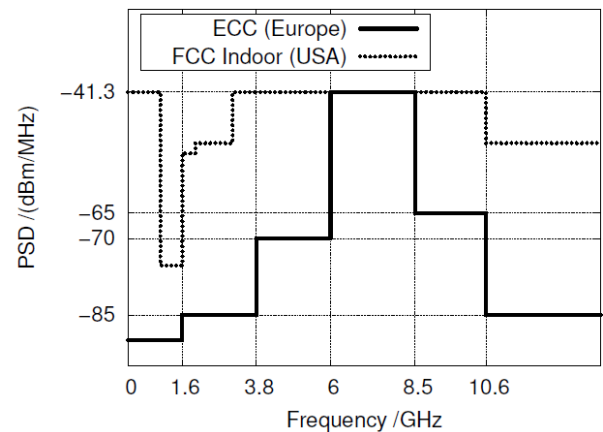


Figure 1. UWB ECC and FCC masks [1]

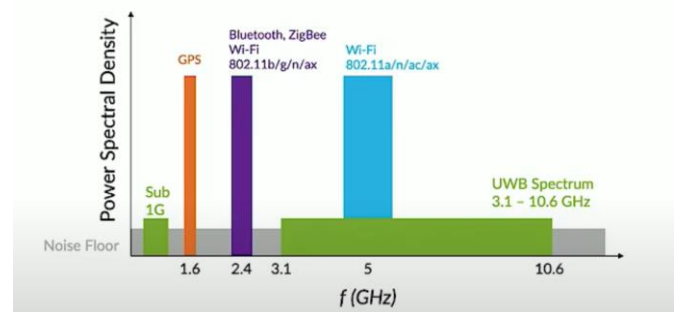


Figure 2. Power spectral density of UWB compared to other technologies [2]

Moreover, UWB is more precise than other RF technologies for location, such as Wi-Fi or Bluetooth Low Energy (BLE), offering accuracy in centimeters resolution instead of meters [3]. This facilitates high precision and low latency in location and ranging applications, as shown in Table I [4], which in turn makes feasible their use in real-time location applications [3] (unlike Wi-Fi and Bluetooth).

TABLE I: COMPARISON OF POSITIONING AND RANGING TECHNOLOGIES [4]

Technology	UWB	Bluetooth	Wi-Fi	RFID	GPS	5G
Precision	1 cm	1-5 m	5-15 m	1 m	5-20 m	10 m
Latency	<1ms	>3 s	>3 s	1 s	100 ms	<1 s

This paper is structured as follows: section II speaks of UWB systems and their features, section III describes the IR-UWB transmitter functional design along with its simulation result, section IV does the same for the IR-UWB receiver. Lastly, the conclusions of this work are presented in section V.

II. UWB: SYSTEMS AND FEATURES

A. Definition of a UWB system

Telecommunication systems can employ different frequency bands according to the bandwidth (BW) used for data transmission. In this way, systems can be classified as narrowband (NB), wideband (WB), and ultra-wideband (UWB), which are defined by considering the lower and upper frequencies of the bandwidth they cover, shown in Fig. 3 and described as [5]

$$\text{NB: } f_H - f_L < 0.01 f_c \quad (1)$$

$$\text{WB: } 0.01 f_c < (f_H - f_L) < 0.2 f_c \quad (2)$$

$$\text{UWB: } f_H - f_L > 0.2 f_c \quad (3)$$

where:

f_c : central frequency of the system

f_L : lower frequency of the bandwidth

f_H : upper frequency of the bandwidth.

The BW of narrowband is less than 1% of its central frequency, the BW of wideband is between 1% and 20%, while the BW of ultra-wideband is greater than 20%.

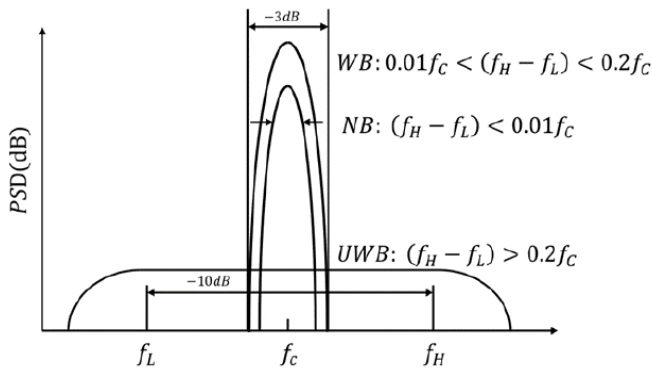


Figure 3. Classification of telecommunications systems based on their bandwidth [5]

Thus, for a system to be classified as UWB, the signal, at any moment, must have a fractional bandwidth of at least 20%, or a bandwidth of at least 500 MHz where the power spectral density of the signal is 10 dB below its maximum density

[6][7]. This means that the bandwidth of a UWB signal is the range of frequencies where its power spectral density drops 10 dB below its maximum value. The definition of a UWB system is independent of the signal shape used [8].

The frequencies above and below the frequency of maximum power density f_M , where this maximum power drops 10 dB, are designated as f_H and f_L respectively, and define the bandwidth of a UWB signal [9].

The 10 dB bandwidths, BW_{10dB} , and the fractional bandwidth μ_{10dB} of an UWB system, are defined in [9] as

$$BW_{10dB} = f_H - f_L \quad (4)$$

$$\mu_{10dB} = \frac{BW_{10dB}}{f_c} \quad (5)$$

$$f_c = \frac{f_H + f_L}{2} \quad (6)$$

where:

f_H : The highest frequency at which the power spectral density of the UWB transmission drops 10 dB relative to f_M

f_M : frequency of maximum power spectral density of the UWB transmission.

f_L : the lowest frequency at which the power spectral density of the UWB transmission drops 10 dB relative to f_M

f_c : central frequency of the 10 dB bandwidth.

B. Main advantages of UWB

The main advantages and features of UWB systems are:

- Ultra-wide bandwidth
- High precision ranging
- Low transmission power (low power consumption)
- Secure communications
- High performance against multipath distortions
- Penetration and localization capabilities
- Resistant to jamming
- Communication system capacity
- Simple transceiver architecture

C. UWB technologies

Wireless UWB systems operating from 3.1 to 10.6 GHz are typically implemented with two broadly used schemes [8]: multiband orthogonal frequency division multiplexing ultra-wide band (MB-OFDM-UWB) and impulse radio ultra-wideband (IR-UWB).

As described in [5], in an MB-OFDM-UWB system, the available UWB spectrum is divided into multiple sub-bands, each with a minimum bandwidth of 500 MHz, using orthogonal frequency division multiplexing (OFDM) in each one. Since the different sub-bands are orthogonal to each other, independent data streams can be transmitted simultaneously without mutual interference within the same spectrum. This design avoids the use of frequencies already employed by other wireless technologies and reduces interference with other systems. Fig. 4 shows the multiband approach used in MB-OFDM-UWB.

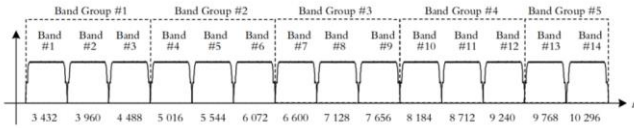


Figure 4. Bands distribution in MB-OFDM-UWB [5]

Impulse Radio Ultra-Wideband (IR-UWB), on the other hand, employs ultra-short pulses (2 ns in duration or less) to transmit information by directly modulating the pulses [5]. Thus, the most basic transmissions of IR-UWB do not need to produce continuous high-frequency carrier waves, as they only need to generate the ultra-short pulses, modulate them, and send them through an antenna.

Reference [8] details that an IR-UWB system transmits and receives a pulse (non-sinusoidal signal) that contains a wide range of frequency components, in which information is transmitted and received using millions of these pulses per second (pulse repetition frequency, PRF), with extremely low power spectral densities across an ultra-wideband spectrum.

An IR-UWB system based on pulses can fully utilize the entire bandwidth from 3.1 to 10 GHz, or it can operate within a specific channel.

D. IR-UWB Transmission Modes

In the IEEE 802.15.4z UWB standard, two physical layers are defined for data transmission according to the PRF: one for low pulse repetition rates (Low-Rate Pulse, LRP UWB) and another for high pulse repetition rates (High-Rate Pulse, HRP UWB). The latter is primarily used in current applications, most of which employ the channels defined from 6 GHz to 10 GHz range with a channel bandwidth of 499.2 MHz [10]. Additionally, it is widely employed in applications requiring low data rate wireless connectivity and precise ranging [11].

The PRF implies that an UWB transmitter will be in standby mode for most of the time without generating pulses, resulting in a low duty cycle and, consequently, low power consumption [12].

The high pulse repetition frequency mode (HPRF), a variant of HRP, includes an encryption mode enabled by a Scrambled Timestamp Sequence (STS), which adds a level of security and accuracy to range measurements, thus providing protection against accidental interference and intentional malicious attacks [13] [14].

The average PRF for LRP is between 1 and 2 MHz, while for HRP it ranges from 3.9 MHz to 249.6 MHz, with a peak PRF that must not exceed 499.2 MHz for each one of the sixteen UWB HRP channels [15].

E. Frequency bands

For the HRP physical layer of UWB, operating frequencies are defined in three different bands, totaling sixteen channels as mentioned previously [15]:

- Band 0 (sub-GHz): consists of 1 channel, occupying the spectrum from 249.6 MHz to 749.6 MHz.
- Band 1 (low band): consists of 4 channels from 3.1 GHz to 4.8 GHz.

- Band 2 (high band): consists of 11 channels, occupying the spectrum from 6.0 GHz to 10.6 GHz.

All these channels use bandwidths ranging from 499.2 MHz to 1.35 GHz. Table II specifies the frequency channel allocation for the HRP UWB physical layer (HRP UWB PHY) [15].

TABLE II: FREQUENCY CHANNEL ALLOCATION FOR HRP UWB PHY [15]

Band	Channel number	Central Frequency (MHz)	BW (MHz)	Mandatory/Optional
0	0	499.2	499.2	Mandatory below 1 GHz
1	1	3494.4	499.2	Optional
	2	3993.6	499.2	Optional
	3	4492.8	499.2	Mandatory in low band
	4	3993.6	1311.2	Optional
2	5	6489.6	499.2	Optional
	6	6988.8	499.2	Optional
	7	6489.6	1081.6	Optional
	8	7488.0	499.2	Optional
	9	7987.2	499.2	Mandatory in high band
	10	8486.4	499.2	Optional
	11	7987.2	1331.2	Optional
	12	8985.6	499.2	Optional
	13	9484.8	499.2	Optional
	14	9984.0	499.2	Optional
	15	9484.8	1354.97	Optional

It is also mentioned in [15], that an HRP UWB device that meets the requirements must be capable of transmitting in at least one of the three specified bands: sub-GHz, low, or high. So, an HRP UWB device implementing the sub-GHz band must implement channel 0. If it implements the low band, it must support channel 3, while the remaining channels in the low band are optional. If it implements the high band, it must support channel 9, with the remaining channels in the high band also being optional.

Table III specifies the frequency channel allocation for LRP UWB PHY established in [16].

TABLE III: FREQUENCY CHANNEL ALLOCATION FOR LRP UWB PHY [16]

Channel number	Central Frequency (MHz)
0	6489.6
1	6988.8
2	7987.2
3	8486.4
4	6681.6
5	7334.4
6	7987.2
7	8640.0
8	9292.8
9	9945.6

F. Modulation types employed in IR-UWB

In IR-UWB, different types of modulation are used to transmit digital data via a sequence of pulses, with information being carried out by directly modifying the

amplitude, duration, and phase of these pulses [5]. The commonly used modulation techniques are [5]:

- Pulse Position Modulation (PPM): Represents binary data by adjusting the position of the pulse within a time interval, where different positions of the pulse within the interval represent different data values.
- Pulse Amplitude Modulation (PAM): Represents binary information by adjusting the amplitude of the pulse, with each different amplitude representing a value of the data to be transmitted.
- On-Off Keying (OOK): The presence or absence of a pulse represents binary data (1 and 0).
- Binary Phase Shift Keying (BPSK): Represents digital information by adjusting the phase of the pulse. A phase of 0° represents a 0, while a phase of 180° represents a 1.

Fig. 5 illustrates these modulation techniques.

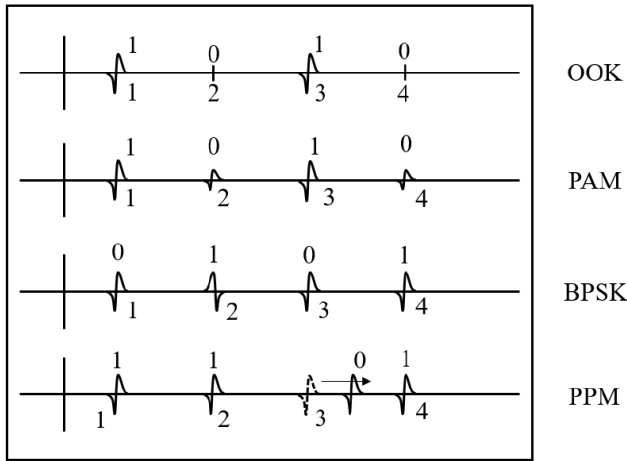


Figure 5. Modulation schemes commonly employed in UWB [5]

- BPM-BPSK Modulation: A combination of burst position modulation (BPM) and BPSK is also used, known as BPM-BPSK modulation, allowing it to be employed in both coherent and non-coherent receivers within a common signaling scheme [15]. Thus, the same system can support both types of receivers. In BPM-BPSK, each symbol can carry two bits of information: one bit determines the position of a burst of pulses, while the second additional bit is used to modulate the phase (polarity) of that same burst [15]. Fig. 6 shows the structure of a BPM-BPSK symbol.

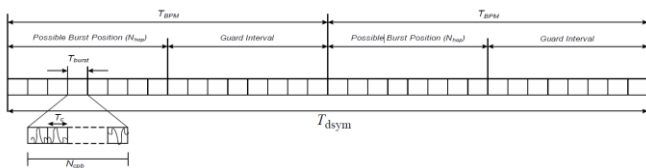


Figure 6. Symbol structure of HRP UWB physical layer [15]

G. UWB types of pulses

The type of pulse to be used in IR-UWB systems is an important factor as it determines the shape of the signal spectrum. In IR-UWB, there are several types of pulse signals that can be employed [8]:

- The step pulse
- The Gaussian pulse
- The single-cycle Gaussian pulse (monocycle)
- The doublet Gaussian pulse
- The multi-cycle pulse
- Rectangular, triangular, and half-cosine pulses [12].

The first derivative of the Gaussian pulse forms the Gaussian monocycle, and the second derivative forms the Gaussian doublet. Thus, for the same pulse duration, higher-order derivatives taken from the Gaussian pulse produce pulses with the same duration but with a higher frequency corresponding to the peak amplitude of the pulse [8].

Among these types of pulses, the Gaussian, monocycle and doublet pulses are typically used [8], though the monocycle is preferred as its frequency spectrum does not contain a direct current (DC) component, thus facilitating simpler wireless transmission. Additionally, it has a broader bandwidth than the multi-cycle pulse and is easier to implement than the doublet [8].

H. Gaussian pulses

As described in [8], the frequency spectrum of Gaussian pulses does not contain secondary lobes beyond the zero-crossing frequency points, which is desirable for signal transmission. The maximum spectral amplitude of the Gaussian pulse occurs at DC, meaning that most of its energy is concentrated at DC and low frequencies near DC. The Gaussian monocycle and the doublet do not contain DC component and have less energy at low frequencies, allowing these pulse shapes to be transmitted more efficiently, resulting in a simpler and more compact design [8].

I. Pulses Spectrum Density

A UWB transmitter must comply with the regional output power spectral density masks, being also important to maximize the use of this PSD, as high spectrum utilization improves communication distance and the range of the IR-UWB positioning system [12].

Equation (7) [12] defines the use of the spectrum in band for a pulse with a signal power $P(f)$, whose total available power $M(f)$ is defined by the UWB spectrum mask, where f_0 is the central frequency of the channel and f_{BW} is its bandwidth.

$$\eta_{in-band} = \frac{\int_{f_0-0.5f_{BW}}^{f_0+0.5f_{BW}} P(f)df}{\int_{f_0-0.5f_{BW}}^{f_0+0.5f_{BW}} M(f)df} \quad (7)$$

Therefore, to achieve high utilization of the UWB spectrum, it is desirable for the main lobe of the channel output spectrum to occupy the power spectral density mask as fully as possible [12].

In theory, the Gaussian pulse has no out-of-band side lobes, while the rectangular pulse has the largest side lobe, which could break the UWB PSD mask requirement [12]. Additionally, pulses with spectral responses including high side lobes energy, such as a rectangular, emit unwanted radiation, which can cause false target detection and/or interference with other existing systems [8]. Therefore, it is desirable to suppress the energy of these secondary lobes. This suppression can be determined by measuring the difference between the power of the main lobe of the channel and that of the secondary lobes.

This article will focus on the functional design of Gaussian, half-cosine, triangular, and rectangular pulse shapes in section III.

J. Methods for generating IR-UWB Pulses

There are various theoretical methods for generating UWB pulses. However, in [8], the use of silicon-based RFIC CMOS (radio frequency integrated circuits) is mentioned as an attractive technology. This approach allows for miniaturization, low cost, and low power consumption, making it suitable for battery-operated systems. Additionally, it can operate at very high frequencies and is easily integrated with digital integrated circuits, which enhances the potential for achieving complete UWB systems on a single chip.

III. FUNCTIONAL DESIGN OF IR-UWB TRANSMITTER

A. IR-UWB FUNCTIONAL TRANSMITTER

Fig. 7 shows the designed schematic for the functional IR-UWB transmitter, taking as reference the architecture from [12], which employs a reconfigurable pulse generator that allows adjustments to the pulse shape.

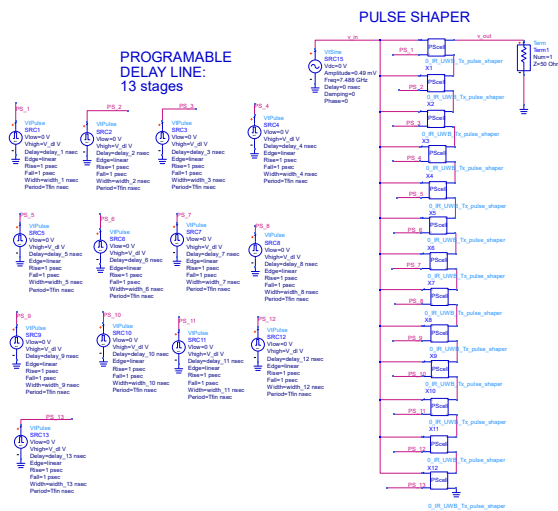


Figure 7. Functional design of the IR-UWB reconfigurable pulse shaper

The design consists of:

- An input RF sine wave signal (v_{in}), at the frequency of the mandatory UWB channel in band 3 of the HRP mode.
- A programmable delay line with 13 stages (or cells), as the optimal number mentioned in [12] for a 28 nm CMOS process.

- A pulse shaper (symbol: PScell) with 13 stages, where each stage is activated by control signals PS_1, PS_2, up to PS_13.

The RF input signal (v_{in}), configured for UWB HRP channel 9 at 7.488 GHz, as shown in Fig. 8, is fed into the input of each stage of the pulse shaper (PS). Simultaneously, each stage of the programmable delay line (PDL) is set to a specific delay time, enabling the RF signal to reach the pulse shaper input after that delay.

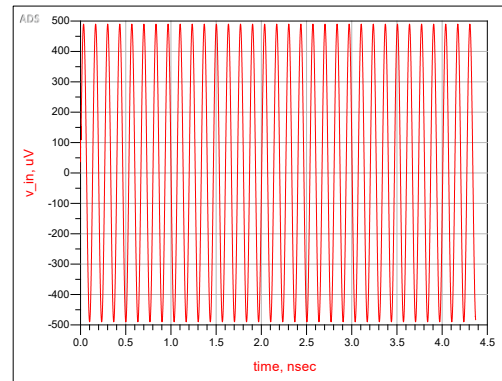


Figure 8. Mandatory RF input signal for UWB channel 9

After the programmed time for each PDL cell has elapsed, the cells generate control signals (PS_1, ..., PS_13) with specific durations, which activate the corresponding stage of the PS. This setup allows each stage to process the RF signal at its input according to the duration of its respective control signal. The output signals from all stages of the PS are then combined to obtain the desired pulse shape, thus enabling specific and symmetric configurations.

Fig. 9 illustrates the design of each cell of the pulse shaper, and Fig. 10 shows its symbol. The pulse shaper consists of a switch that is activated by the corresponding control signal from the PDL, followed by a voltage-controlled voltage source (VCVS) with unit functional gain, which acts as a voltage follower. All stages of the PS are connected from their output terminal, "Out Num 3", to the interconnection terminal, "Interconnection Num=4", of the next stage, to combine their signals at the output of the pulse shaper (v_{out}).

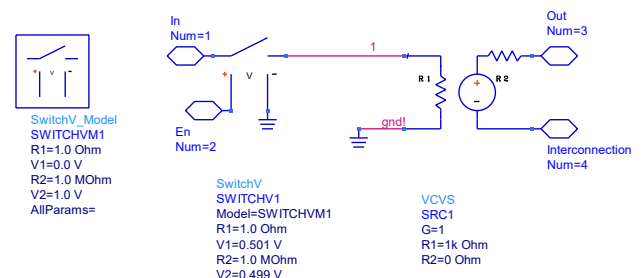


Figure 9. Internal implementation of the pulse shaper (PS)

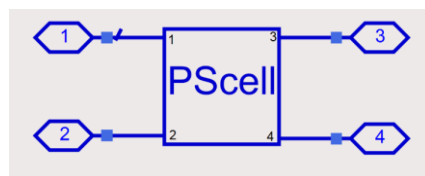


Figure 10. Pulse shaper symbol

B. Simulation results

The design of a Gaussian pulse with a 3.7 ns width and a bandwidth of 500 MHz is referenced from [12]. Thus, for 13 delay stages, an average sampling period of the RF input signal is established to conform the UWB pulse shape, as follows

$$\tau = \frac{3.7 \text{ ns}}{2 * N_{etapas} - 1} = \frac{3.7}{25} = 148 \text{ ps.}$$

Fig. 11 illustrates the four types of pulses generated.

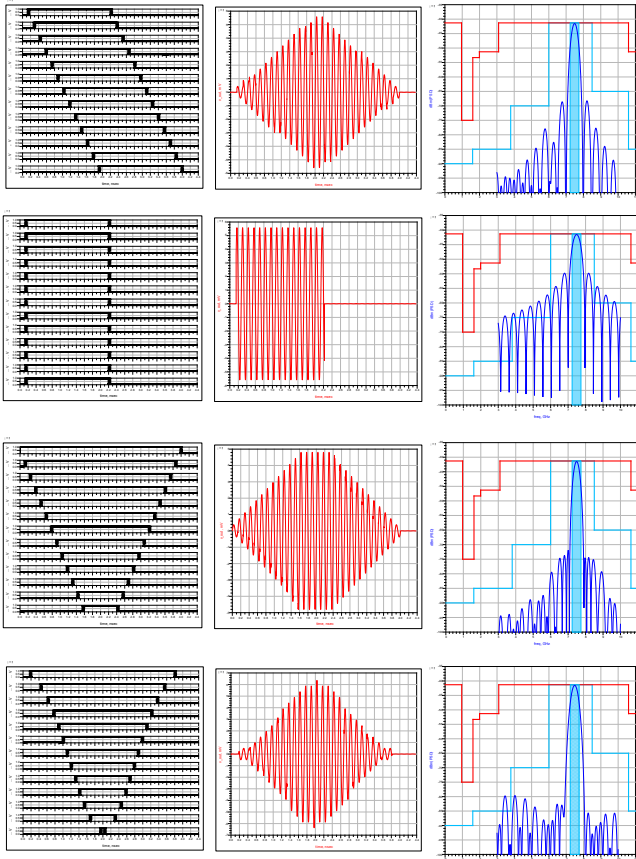


Figure 11. Pulse shapes generated, and its PSD

From the first to the fourth row, the triangular, rectangular, half-cosine and Gaussian pulses are displayed, in that order. Each row shows, from left to right, the width of the control signals for each of the 13 delay stages in the PDL, the resulting pulse shape in the center, and the corresponding power spectral density on the right. The red line defines the UWB mask according to the FCC, while the blue line represents the UWB mask according to the ECC.

Table IV summarizes the results obtained from the functional simulations, where it can be noted that to achieve similar levels of bandwidth efficiency at a 500 MHz bandwidth, the Gaussian pulse requires the highest input voltage but offers the best side lobe suppression. In contrast, the half-cosine pulse achieves the same spectral efficiency with the lowest input voltage, while still maintaining good side lobe suppression. The rectangular pulse performs the worst in this regard, and the triangular pulse offers acceptable performance, requiring less input voltage than the Gaussian pulse.

TABLE IV: SPECTRAL EFFICIENCY AND SIDELobe SUPPRESSION ACHIEVED WITH SIMULATED PULSES

Pulse type	Input voltages (mV)	In band efficiency for 500 MHz BW (%)	Sidelobe supression (dB)	Pulse width (ns)
Triangular	0.43	94.86	26.73	3.85
Rectangular	0.43	94.85	13.28	2
Half-cosine	0.37	95.49	30.46	4
Gaussian	0.49	94.97	41.09	3.62

Additionally, except for the rectangular pulse, all pulse shapes comply with the FCC and ECC masks within the channel width. The lobes extending beyond the channel that exceed the ECC mask can be fully suppressed through additional filtering. For the Gaussian pulse, the bandwidth corresponding to a 10 dB attenuation relative to the main lobe's maximum power is $BW_{10dB} = 637 \text{ MHz}$.

IV. FUNCTIONAL DESIGN OF IR-UWB RECEIVER

In this section, the functional design of the proposed IR-UWB receiver architecture is presented taking as reference the architecture from [17].

Fig. 12 shows the block diagram of the functional design of the IR-UWB receiver.

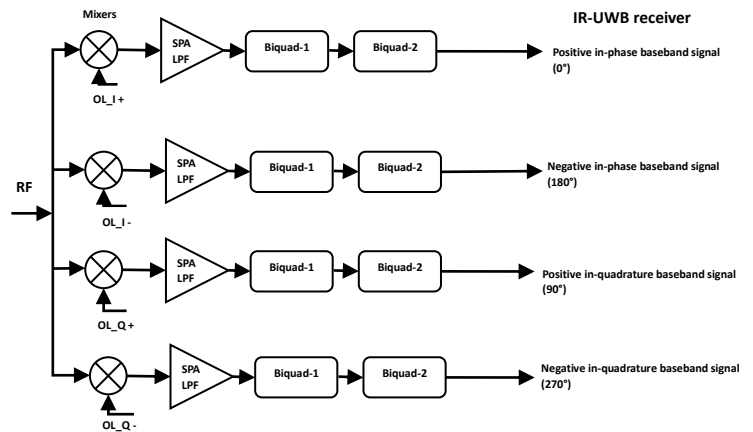


Figure 12. IR-UWB receiver block diagram

The receiver architecture design focuses on the components of the 5th-order Gaussian filter to 6 dB, aiming to achieve a flat group delay across the entire frequency range of interest. In indoor positioning applications, a constant or flat group delay ensures that the receiver does not distort the measured time delay, thereby preserving the accuracy of the object's location.

The architecture designed of the 5th-order Gaussian filter to 6 dB consists of a single pole active low pass filter, (SPA-LPF), cascaded with a two-stage biquad filter.

A. Cutoff Frequencies computation for the 5th-Order Gaussian Filter to 6 dB

For the design of the SPA-LPF and the two biquad stages, it is necessary to select their respective cutoff frequencies to form the 5th-order Gaussian filter to 6 dB. The target baseband frequency is 249.6 MHz, and the cutoff frequencies for each stage of the 5th-order to 6 dB Gaussian filter are

shown in Table V, computed using Gaussian to 6 dB design table in [18]. SPA-LPF represents stage 1 and stages 2 and 3 are the biquads.

TABLE V: CUTOFF FREQUENCIES AND QUALITY FACTOR FOR EACH STAGE OF 5TH-ORDER GAUSSIAN FILTER TO 6 DB [17]

Section	f_0 (MHz)	Q
SPA-LPF	166.25	-
Biquad 1	257.93	0.83
Biquad 2	402.18	2.26

B. 5th-Order Gaussian Filter to 6 dB

Fig. 13 illustrates the design of the 5th-order Gaussian filter to 6 dB, and Fig. 14 its symbolic representation. The SPA-LPF is in inverting mode with feedback capacitor value $C=1.485$ pF. In the biquads the voltage-controlled current sources represent the transconductors, terminal v_{in} represent its input, terminal v_{bp} represents a bandpass response while terminal v_{lp} represents a low-pass response. The input of the SPA-LPF represents the input of the Gaussian filter, its output is directly connected to the input of BIQUAD_1, while the low-pass output of BIQUAD_1 is connected to the input of BIQUAD_2. The low-pass output of BIQUAD_2 represents the output of the Gaussian filter.

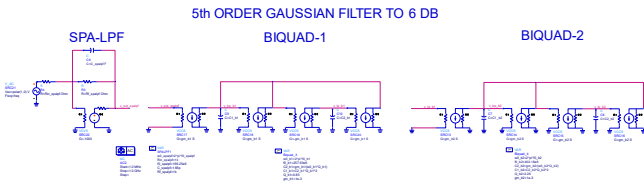


Figure 13. Functional design for 5th-order Gaussian filter to 6 dB

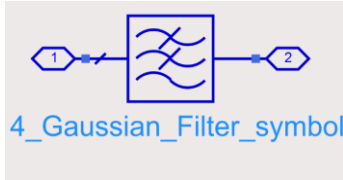


Figure 14. Symbol of 5th-order Gaussian filter to 6 dB

C. Functional Design of IR-UWB Receiver

Fig. 15 displays the functional design of the IR-UWB receiver. The local oscillator circuit generates reference signals at four different phases (0° , 90° , 180° , 270°). The input signal (v_{in}) is split into four branches, where each one is mixed with the reference signals from the local oscillator, to generate in-phase and quadrature signals in differential mode. Then, in each branch, the signals pass through the designed fifth-order Gaussian filter to 6 dB to deliver the desired baseband frequency of 249.6 MHz at its output. Finally, the differential signals are combined to obtain the desired output signals in phase and quadrature. The simulation is conducted on the mandatory frequency channel of the high band in HRP UWB mode, channel 9 at 7.9872 GHz.

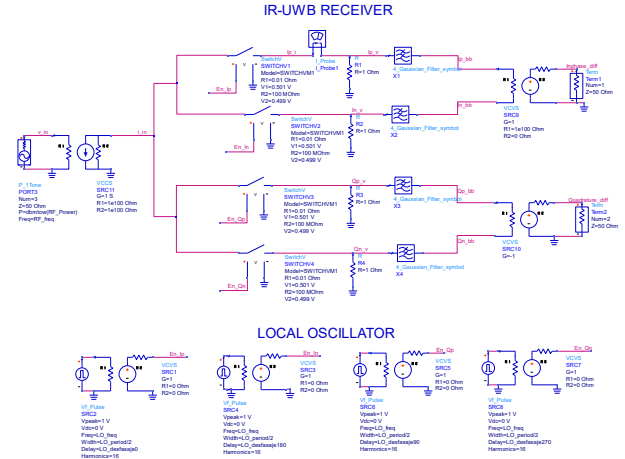


Figure 15. Functional implementation of IR-UWB receiver

D. SIMULATION RESULTS

Fig. 16 shows the group delay for the mandatory UWB channel 9, highlighting that it maintains a nearly constant value across the entire frequency range at the baseband frequency of 249.6 MHz.

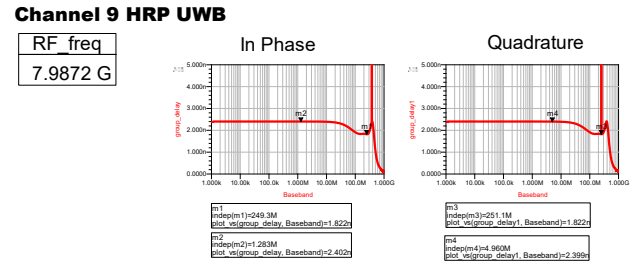


Figure 16. Group delay of in phase and quadrature output signals for HRP UWB channel 9

Fig. 17 shows the receiver's conversion gain (CG) curve for the in-phase output signal, which exhibits a shape similar to that of a 5th-order Gaussian filter to 6 dB [17]. The 6 dB attenuation occurs at the receiver's cutoff frequency of 249.6 MHz (marker m7 = 250.2 MHz on the graph).

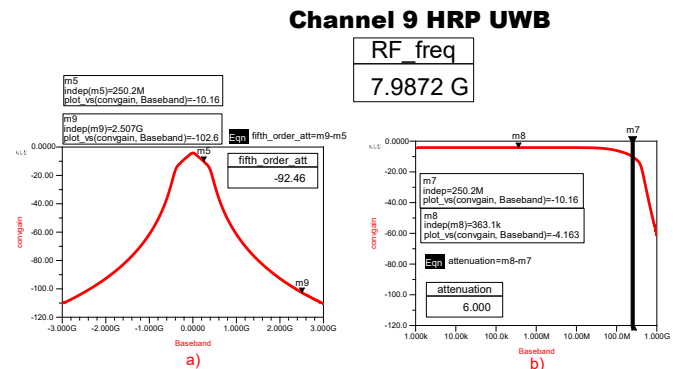


Figure 17. Conversion gain for in phase output signals of HRP UWB channel 9

For comparison purposes, Figures 18 and 19 shows the group delay and frequency response, in that order, for a feedback capacitor value of 0.957 pF used in the SPA-LPF, instead of the 1.485 pF value that produced the results in Figs. 16 and 17. It can be noted that the group delay is completely flat across the entire baseband of interest, at the expense that the frequency response has lower rejection slope, being the attenuation at the cutoff frequency of 3 dB instead of 6 dB. This suggests that the feedback capacitor value at the SPA-

LPF stage can be adjusted as needed, to provide a full pulse shape preservation, or to improve out-of-band filtering, but not both simultaneously. It is important to note that in indoor positioning applications, a constant group delay ensures the receiver will not distort the measured time delay, thereby preserving the accuracy of the object's location. Nonetheless, a feedback capacitor value that achieves 6 dB attenuation at the Gaussian filter's cutoff frequency provides the theoretically optimal balance between pulse shape preservation and out-of-band filtering, as stated in [17].

Channel 9 HRP UWB

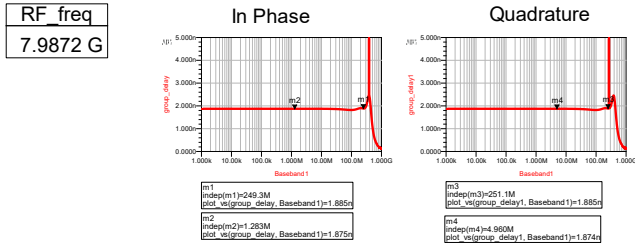


Figure 18. Group delay response for feedback capacitor of SPA-LPF stage, equal to 0.957 pF

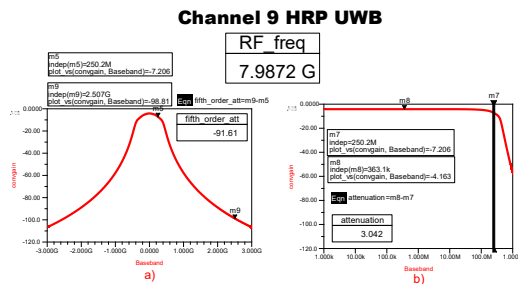


Figure 19. Conversion gain response for feedback capacitor of SPA-LPF stage, equal to 0.957 pF

V. CONCLUSIONS

In this article, an analysis of transmission and reception systems was conducted to functionally implement an IR-UWB transmitter and receiver in compliance with the IEEE 802.15.4z standard for indoor positioning applications. For the transmitter, various pulse shapes were designed, with the Gaussian pulse standing out for its efficient use of the spectrum as well as high sidelobes suppression, achieving a level of 41.09 dB. Additionally, the half-cosine pulse required the lowest input voltage to achieve the same spectral efficiency, while also providing a commendable level of sidelobe suppression equal to 30.46 dB. For the designed receiver architecture, a flat frequency response was obtained at baseband, along with a nearly constant group delay across the entire baseband, which is a crucial factor in precise ranging applications. Furthermore, it was verified that the feedback capacitor of SPA-LPF stage can be adjusted to optimize either the group delay response, or out-of-band filtering, but not both simultaneously.

REFERENCES

[1] B. Schleicher and H. Schumacher, "Impulse generator targeting the European UWB mask," 2010 Topical Meeting on Silicon Monolithic Integrated Circuits in RF Systems (SiRF), New Orleans, LA, USA, 2010, pp. 21-24, doi: 10.1109/SMIC.2010.5422846.

[2] Cooper, S., Wireless LAN Professionals, 4 de marzo de 2020, Ultra-Wideband & You | Stephen Cooper CWNE #276 | WLPC Phoenix 2020 | @Stephen_Cooper. YouTube link video: <https://youtu.be/TR-rahY3Y2k>

[3] "Getting Back to Basics with Ultra-Wideband (UWB)" Qorvo, White Paper, May 2021. Link: www.qorvo.com

[4] "Introducción a ultra-wideband", MathWorks, Link: <https://es.mathworks.com/discovery/ultra-wideband.html>

[5] C. Zheng, Y. Ge, y A. Guo, "Ultra-Wideband Technology: Characteristics, Applications and Challenges", arXiv:2307.13066v2 [eess.SP], Aug. 13 2023. Link: <https://doi.org/10.48550/arXiv.2307.13066>

[6] Federal Communications Commission, "Revision of Part 15 of the Commission's Rules Regarding Ultra-Wideband Transmission Systems," Second Report and Order and Second Memorandum Opinion and Order, FCC 04-285, Dec. 2004. Link: <https://www.fcc.gov/document/revision-part-15-commissions-rules-regarding-ultra-wideband-1>

[7] International Telecommunication Union, "Measurement techniques of ultra-wideband transmissions," Recommendation ITU-R SM.1754-0, 2006.

[8] Nguyen, C., & Miao, M., "Design of CMOS RFIC Ultra-Wideband Impulse Transmitters and Receivers", Springer, 2017, Link: <https://doi.org/10.1007/978-3-319-53107-6>

[9] International Telecommunication Union, "Characteristics of ultra-wideband technology," Recommendation ITU-R SM.1755-0, 2006.

[10] "Ultra-wideband (UWB) LPF communication and ranging", Rohde & Schwarz USA, Inc. (2024). Link: https://www.rohde-schwarz.com/us/solutions/test-and-measurement/wireless-communication/wireless-connectivity/ultra-wideband/ultra-wideband-overview_253919.html#gallery-9

[11] "802.15.4 UWB Concepts", N7610C Signal Studio for IoT 2025 Online Documentation, Software version 4.4, Help revised 7/18/2024, Keysight Technologies, Inc., 2018-2024. Link: <https://helpfiles.keysight.com/csg/n7610/Content/Main/Concept%20802.15.4%20UWB.htm#:~:text=UWB%20Channel%20Assignment,use%20of%20variable%2Dlength%20bursts.>

[12] H. Chen, Z. Chen, R. Ou, R. Chen, Z. Wu and B. Li, "An IEEE 802.15.4z-Compliant Reconfigurable Pulse-Shaping UWB Digital Power Amplifier in 28-nm CMOS," in IEEE Transactions on Microwave Theory and Techniques, vol. 71, no. 10, pp. 4366-4376, Oct. 2023, doi: 10.1109/TMTT.2023.3263898

[13] "Ultra-wideband testing: Practical introduction to UWB measurements", LitePoint, A Teradyne Company, Doc: 1075-0607-001, March 2020 Rev 1, Link: <https://mcs-testequipment.com/content/files/Testing-UWB-Whitepaper-031620-web.pdf>

[14] Hsu, E. , "An overview of the IEEE 802.15.4 HRP UWB standard", Keysight Technologies, July 28, 2021, Link:

<https://www.keysight.com/blogs/en/tech/rfmw/2021/07/28/an-overview-of-the-ieee-802154-hrp-uwband-standard>

[15] "IEEE Standard for Low-Rate Wireless Networks", in IEEE Std 802.15.4-2020 (Revision of IEEE Std 802.15.4-2015), pp.1-800, 23 July 2020, doi: 10.1109/IEEESTD.2020.9144691.

[16] "IEEE Standard for Low-Rate Wireless Networks--Amendment 1: Enhanced Ultra-Wideband (UWB) Physical Layers (PHYs) and Associated Ranging Techniques," in IEEE Std 802.15.4z-2020 (Amendment to IEEE Std 802.15.4-2020), pp.1-174, 25 Aug. 2020, doi: 10.1109/IEEESTD.2020.9179124.

[17] M. Song et al., "A Low-Power 6–9-GHz IEEE 802.15.4a/4z Compliant IR-UWB Transceiver With Pulse Pre-Emphasis Achieving High ToA Precision," in IEEE Solid-State Circuits Letters, vol. 6, pp. 297-300, 2023, doi: 10.1109/LSSC.2023.3335596.

[18] H. Zumbahlen and Analog Devices, (2008), "Linear Circuit Design Handbook", 1st ed., Burlington, MA, USA: Elsevier, pp. 621. ISBN: 978-0-7506-8703-4.